Received July 31, 2017, accepted August 21, 2017, date of publication August 29, 2017, date of current version October 12, 2017.

Digital Object Identifier 10.1109/ACCESS.2017.2745705

Interval Non-Probabilistic Reliability of a Surrounding Jointed Rockmass in Underground Engineering: A Case Study

LONGJUN DONG[1,2], (Member, IEEE), DAOYUAN SUN[1], XIBING LI[1], AND ZILONG ZHOU[1]
[1]School of Resources and Safety Engineering, Central South University, Changsha 410083, China
[2]Jiaojia Gold Mine, Shandong Gold Group Co. Ltd., Laizhou 261441, China

Corresponding author: Longjun Dong (lj.dong@csu.edu.cn)

This work was supported in part by the National Basic Research Program of China under Grant 2015CB060200, in part by the National Natural Science Foundation of China under Grant 41630642 and Grant 51504288, in part by the China Postdoctoral Science Foundation under Grant 2015M570688 and Grant 2016T90639, in part by The Young Elite Scientists Sponsorship Program by CAST under Grant 2016QNRC001, and in part by the Innovation-Driven Project of Central South University under Grant 2016CXS001.

ABSTRACT To consider the uncertainty when determining the values of geo-mechanical parameters, interval values are used to indicate the physical and mechanical parameters of the rockmass. An interval non-probabilistic reliability model of the surrounding jointed rockmass of an underground opening, which can be used when the data are scarce, is developed to evaluate the stability of the rockmass in the Jiaojia gold mine. The calculation results of the interval non-probabilistic reliability are in agreement with the actual situation. Thus, the interval non-probabilistic reliability is a beneficial complement to the traditional analysis methods of the random reliability and the safety factor.

INDEX TERMS Underground engineering, jointed rockmass, block theory, interval non-probabilistic reliability.

I. INTRODUCTION

During the excavation of mines and tunnels, rockmasses are divided into blocks of different sizes and forms by structural planes. The blocks that are exposed to the free surface will slide along the structural planes and will no longer be in a balanced state, resulting in a chain reaction that causes local instability. Thus, it is important to investigate the stability characteristics of a rockmass [1]–[3]. Block theory [1], [3] was proposed by Goodman and Shi. As one of the most effective methods to analyze block stability, the theory has been widely used and discussed in rock mechanics and engineering.

In the design of a mining system, the stability level of the surrounding jointed rockmass in underground engineering is typically expressed by a safety factor, which is defined as the ratio of the integral of the characteristic shear strength to the driving forces (gravitational) over the critical failure surface. However, 'high' safety factors do not necessarily denote low probabilities of failure [1]–[7]. Duncan [8] reported that, through regulation or tradition, the same safety factor was often applied to conditions that involved varying degrees of uncertainty; A bootstrap method was proposed by Li et al. for characterizing the effect of uncertainty in shear strength parameters on slope reliability [9].

Recent interest and the application of load and resistance factor design methods have allowed engineers to implicitly account for uncertainties using statistical methods and random field theory [4], [5], [8], [10]–[15]. Orr [16] traced the changes that have occurred in how the parameter values for use in geotechnical designs have been defined and selected, and discussed what changes have been proposed for the revision of Eurocode 7 to make the selection of characteristic soil parameter values more objective. Fenton and Griffiths [17] developed the random finite-element method (RFEM), which combined nonlinear finite-element methods with random field generation techniques. Subsequently, the RFEM was further developed to combine three-dimensional elastoplastic finite elements and three-dimensional random field theory in the Monte Carlo framework to directly assess the influences of the coefficient of the variation of soil strength and the spatial correlation length on the slope reliability [18], [19]. Jiang *et al.* [20] developed an approach for efficient evaluation of the system failure probability P_f, of slope stability in spatially variable soils based on Monte Carlo simulation.

Li *et al.* [21] presented one approach to evaluate the uncertainty in safety factor and P_f of slope in the presence of geological uncertainty using borehole data. Tan *et al.* [22] suggested that the utilization of the approximate response surface functions for a reliability assessment can reduce the computational costs in structural reliability analysis. Li *et al.* [23] reviewed previous literature on developments and applications of response surface methods in different slope reliability problems, and identified soil slope reliability analysis problems into four types. Lü and Low [24] performed a probabilistic analysis of underground rock excavations using the response surface method and the second-order reliability method, in which the quadratic polynomial with cross terms was used to approximate the implicit limit state surface at the design point. Low *et al.* [25] provided a short code in the ubiquitous Excel spreadsheet platform for efficiently calculating the bounds of the system failure probability. Dadashzadeh *et al.* [26] proposed an integrated methodology for probabilistic numerical modeling of rock slope stability based on response surface method, in which FORM was used to develop an explicit performance function from the results of numerical simulations.

Despite the great achievements reported in the literature on the reliability analysis method based on probability theory, some difficulties remain in the applications of rock mechanics and mining engineering. First, for probabilistic reliability analysis on the stability of the surrounding rock, the distribution form of the parameter must be ascertained, which is a difficult task when the exploration of the sampling points and test data are both scarce. Moreover, presumptions of the probability distribution forms cannot be applied in all circumstances, and reliability indexes corresponding to different forms differ considerably [5], [27]. Second, when the amount of data is scarce [27], minor errors caused by the censored data of the distribution function inevitably lead to an unacceptable analytical result of the reliability index because the probabilistic reliability analysis model is highly sensitive to this parameter value. Thus, a method for efficiently analyzing the reliability of surrounding rock, even with scarce data, must be established.

The calculation parameters in the stability analysis of the surrounding rock take on different degrees of uncertainty due to the heterogeneity of the rockmass in underground caverns, the discreteness of the surveying sampling points and the randomness of the load. The interval non-probabilistic reliability analysis methods for structures [28]–[36] based on interval theory provide a useful approach to evaluate these uncertainties. Interval values can reflect the uncertainty of a parameter value when the number of samples is scarce, thus reducing the demand for data information. In a project study, it is easier to determine the range of a mechanical parameter than to determine both the exact value and the probability distribution of the parameter. Therefore, the paper focuses on how to evaluate the stability of a jointed rockmass in an underground cavern using the interval non-probabilistic reliability analytical method and presents a reasonable application of the interval strength to analyze the stability of the underground jointed rockmass in caverns.

Consequently, interval values are adopted as the parameter values according to interval mathematical theory. Dong and Li [37] adopted the interval rock strength to reflect the uncertainty of the reliability based on an analysis of the characteristics of the parameter values. A comprehensive reliability analysis method of the surrounding rock in underground caverns was established by investigating the research method of the interval non-probabilistic reliability. To further improve and perfect theories and methods of reliability analysis for underground caverns, the calculated results were compared with the results obtained from the methods of random reliability and the safety factors.

II. LIMIT STATE EQUATION AND SLIDING CHARACTERISTICS OF ROCK BLOCKS

Structural planes in a rockmass affect the deformation and damage of a jointed rockmass. The principles of establishing a reliability model of a jointed rockmass in an underground cavern are as follows. First, all of the infinite fractured blocks should be determined according to stereographic projection and vector analysis theory; next, all of the removable and key blocks should be determined; finally, mechanical analysis of the key blocks should be combined with the reliability method to obtain the performance function and establish an analytical model for the reliability of the jointed rockmass.

It is not difficult to determine the faults and occurrence of a large-scale structural plane in a practical project; thus, these parameters can be regarded as a constant value in the calculation. Reliability modeling only considers the uncertainty of the mechanical parameters of a rockmass.

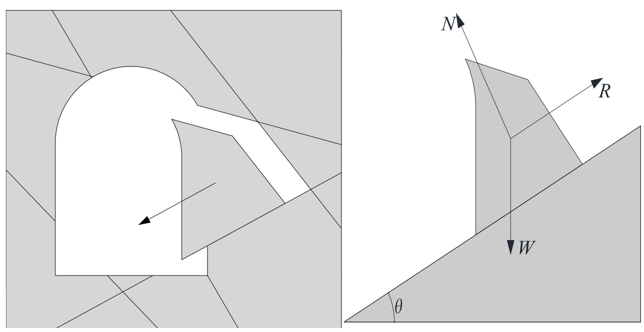

FIGURE 1. **2D figure of a block sliding along a single structural plane: *W*, *R* and *N* indicates the gravity, the resistance force, and the supporting force, respectively.**

A. SLIDING ON A SINGLE STRUCTURAL PLANE

When a block sliding along a single block i, the strained condition of the block is shown in Fig. 1. To analyze the state condition of the block, the forces are resolved into the sliding direction and the direction normal to the plane.

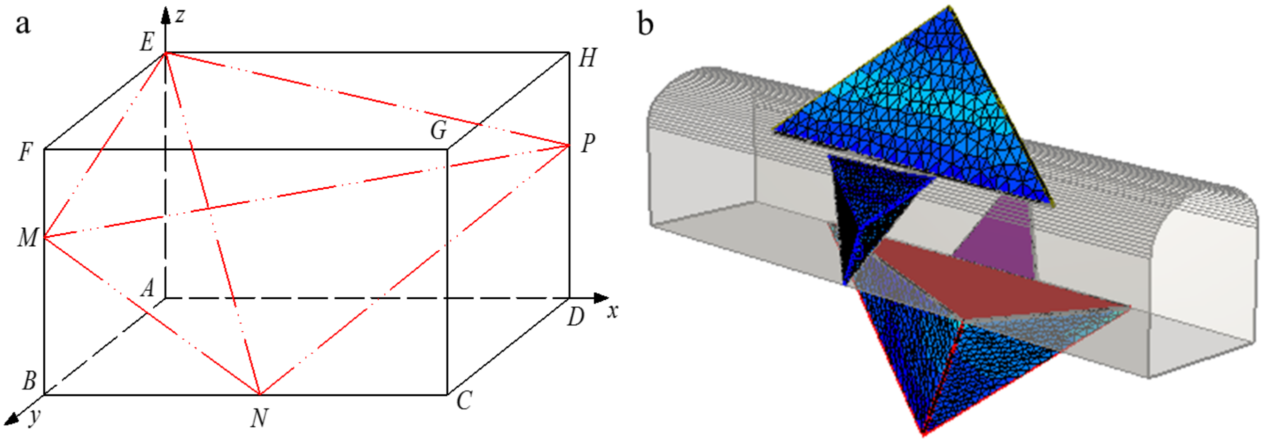

FIGURE 2. Sketch of a block sliding along two structural planes (a the sketch map of a block sliding along two structural planes; b the formed blocks in an actural tunnel).

In the direction normal to the structural plane, the total force can be expressed as equation (1)

$$N = W\cos\theta \tag{1}$$

Along the sliding direction, the active force S and the resistance force R are shown in equation (2) and equation (3)

$$S = W\sin\theta \tag{2}$$

$$R = N\tan\varphi + cs \tag{3}$$

where θ, W, N, φ, c, and s indicate the angle of the sliding direction to the horizontal plane, the gravity, the normal force to the structural plane, the internal frictional angle, the cohesive strength, and the area of the sliding plane, respectively.

While a key block is sliding along a single joint plane, the limit state equation can be defined as equation (4)

$$R - S = W\cos\theta\tan\varphi + cS - W\sin\theta \tag{4}$$

B. SLIDING ON TWO STRUCTURAL PLANES

When a block slides along two structural planes i and j, except for sliding plane i and j, other structural planes are all detached from the sliding block. As shown in Fig. 2, when the block *EMNP* sliding along two structural planes *EMN* and *EPN*, the sliding direction is the intersection line *EN*. Note the dip directions of the two structural planes as α_1, α_2, and the dip angles as β_1, β_2. The normal vectors of the two structural planes can be expressed as $\overrightarrow{n_1} = (\sin\alpha_1\sin\beta_1, \sin\alpha_1\cos\beta_1, \cos\alpha_1)$ and $\overrightarrow{n_2} = (\sin\alpha_2\sin\beta_2, \sin\alpha_2\cos\beta_2, \cos\alpha_2)$, therefore, the direction of the intersection line *EN* can be noted as $\vec{d} = \overrightarrow{n_1}\times\overrightarrow{n_2}$.

The gravity is also projected into the three directions and shown in equations (5) to (7).

$$\overrightarrow{W_d} = \vec{W}\cdot\frac{\vec{d}}{\left|\vec{d}\right|} = \left|\vec{W}\right|\cos\left\langle\vec{W}, \vec{d}\right\rangle \tag{5}$$

$$\overrightarrow{W_{n_1}} = \vec{W}\cdot\frac{\overrightarrow{n_1}}{\left|\overrightarrow{n_1}\right|} = \left|\vec{W}\right|\cos\left\langle\vec{W}, \overrightarrow{n_1}\right\rangle = N_1 \tag{6}$$

$$\overrightarrow{W_{n_2}} = \vec{W}\cdot\frac{\overrightarrow{n_2}}{\left|\overrightarrow{n_2}\right|} = \left|\vec{W}\right|\cos\left\langle\vec{W}, \overrightarrow{n_2}\right\rangle = N_2 \tag{7}$$

The active force S and the resistance R along the sliding direction can be expressed as equation (8) and equation (9), and the limit state equation can be written as equation (10).

$$S = W_d = \left|\vec{W}\right|\cos\left\langle\vec{W}, \vec{d}\right\rangle = W\sin\theta \tag{8}$$

$$\begin{aligned} R &= R_1 + R_2 = \overrightarrow{W_{n_1}}\tan\varphi_1 + c_1 s_1 + \overrightarrow{W_{n_2}}\tan\varphi_2 + c_2 s_2 \\ &= N_1\tan\varphi_1 + c_1 s_1 + N_2\tan\varphi_2 + c_2 s_2 \end{aligned} \tag{9}$$

$$R - S = N_1\tan\varphi_1 + N_2\tan\varphi_2 + c_1 s_1 + c_2 s_2 - W\sin\theta \tag{10}$$

where $\overrightarrow{W_d}$, $\overrightarrow{W_{n_1}}$, $\overrightarrow{W_{n_2}}$ indicate the component of the gravity along the direction of the intersection line of the two structural planes, and the components of the gravity pointed to the two structural planes; N_1, N_2 indicate the normal force to the two structural planes; φ_1, φ_2, c_1, c_2, s_1 and s_2 indicate the internal frictional angle, the cohesive strength, and the area of the two structural planes, respectively.

III. PROBABILISTIC RELIABILITY METHOD FOR BLOCK STABILITY

Consider a removable block sliding on two structural planes to define the random reliability. Suppose the limit state function of a removable block in the following form:

$$g(\boldsymbol{X}) = g(c_1, c_2, \varphi_1, \varphi_2) \tag{11}$$

where $\boldsymbol{X} = (c_1, c_2, \varphi_1, \varphi_2)$ are the random variables. The failure surface can be expressed as $g(\boldsymbol{X}) = 0$ and it divides the variable space into the failure domain and the safe domain. The reliability of a block can be defined as

$$P_s = 1 - P_f \tag{12}$$

where P_f is the failure probability. The reliability index can be obtained as follows:

$$\beta = \frac{\mu_g}{\sigma_g} \tag{13}$$

where μ_g is the mean of $g(\boldsymbol{X})$, σ_g is the standard deviation of $g(\boldsymbol{X})$. The random reliability of a block can be expressed as

$$P_s = 1 - \Phi(-\beta) = \Phi(\beta) \tag{14}$$

where Φ is the standard normal distribution function, β is the reliability index.

The random reliability is used to describe the probability of a unit to perform its intended functions under stated operating conditions for a specified period of time. As defined above, random reliability provides us a standard to evaluate the reliability of a certain block, i.e. the block is reliable if the random reliability is near to 1 while the structure is unreliable if the random reliability is much less than 1, and measures should be taken to guard against accidents.

IV. SYNTHESIZED INTERVAL NON-PROBABILISTIC RELIABILITY METHOD FOR BLOCK STABILITY

Uncertainty theory has developed rapidly and has been widely applied in recent years. Ben-Haim *et al.* [33] proposed the uncertainty convex model to address the deficiencies of the probabilistic model. Subsequently, Guo *et al.* [34] established a theoretical interval non-probabilistic reliability model for evaluating the reliability of structures. In this paper, the theory of interval non-probabilistic reliability was used to analyze the reliability of blocks. The interval non-probabilistic reliability η of a block is defined as the minimum distance of the normalized failure surface from origin of $\mathbb{C}^n$, and the distance is measured in l_∞ norms. $\eta = 1$ means that the most probable failure point is located on the boundary of failure domain, and the reliability of rockmass structure has reached a critical state. For the case of $0 \le \eta < 1$, some combinations of uncertain parameters may be out of the reliable domain. The rockmass structure or system cannot satisfy the reliability requirement. When $\eta > 1$, all possible points of the rockmass structure lie into the reliable domain, and the rockmass structure is safe and reliable. To guarantee the safety of rockmass structures and obtain adequate safety margin, the interval non-probabilistic reliability η can be chosen to be larger than 1.

The interval values of the shear strength parameters of a rockmass are $[c^l, c^u]$, and $[\varphi^l, \varphi^u]$. Suppose that the interval non-probabilistic reliability of the jointed rockmass in an underground cavern is η. When $\eta > 1$, the jointed rockmass in an underground cavern is reliable; otherwise, it is unreliable. A larger value of η indicates a higher level of reliability. An interval non-probabilistic reliability solution method should be further established using the method described above to analyze the reliability comprehensively. The friction coefficient can be written as $f_i = \tan\varphi_i$, for convenience of analysis, according to the interval standardize method, the interval limit state equation (4) and equation (10) can be written as the standard form in equation (15) and equation (16).

$$\begin{aligned} Z_1 = R - S = W\cos\theta\left(f_1^c + f_1^r \delta_{f_1}\right) \\ + \left(c_1^c + c_1^r \delta_{c_1}\right) S - W \sin\theta \end{aligned} \tag{15}$$

$$\begin{aligned} Z_2 = R - S = N_1\left(f_1^c + f_1^r \delta_{f_1}\right) + N_2\left(f_2^c + f_2^r \delta_{f_2}\right) \\ + \left(c_1^c + c_1^r \delta_{c_1}\right) S_1 + \left(c_2^c + c_2^r \delta_{c_2}\right) S_2 - W \sin\theta \end{aligned} \tag{16}$$

where $(f_i^c + f_i^r \delta_{f_i})$, $(c_i^c + c_i^r \delta_{c_i})$ and $(f_j^c + f_j^r \delta_{f_j})$, $(c_j^c + c_j^r \delta_{c_j})$ are the interval shear strengths of structural planes i and j, $\delta_1 = [\delta_{f_i}, \delta_{c_i}]$ and $\delta_2 = [\delta_{f_i}, \delta_{c_i}, \delta_{f_j}, \delta_{c_j}]$ are the standardized interval value vectors; $c_i^c = (c_i^l + c_i^u)/2$, $c_i^r = (c_i^u - c_i^l)/2$, $[c_i^l, c_i^u] = c_i^c \pm c_i^r \delta_{c_i}$, $\delta_c \in [-1, 1]$, and similar parameters are assigned to the other planes.

According to the non-probabilistic reliability theory, the equations of the interval non-probabilistic reliability [13] η_m ($m = 1, 2$) for the standardized interval performance functions (15) and (16) can be solved as

$$\eta_m = \min\{\|\boldsymbol{\delta}_m\|_\infty\} \tag{17}$$

and meet the condition

$$Z_m = g(\boldsymbol{\delta}_m) = 0 \tag{18}$$

To establish a method for solving the interval non-probabilistic reliability η_m, based on previous studies, Jiang *et al.* [35] proposed an one-dimensional optimization algorithm that can effectively avoid interval extension when calculating the complex performance function. The paper will apply this method to solve the interval non-probabilistic reliability. The specific analysis process is described below.

(1) Consider a block sliding along a single structural plane first. List 2 super radiation lines/ultra-rays that pass through the origin $O_{\delta_1}^\infty = \{\boldsymbol{\delta}_1 : \delta_{1k} = 0, k = 1, 2\}$ of the δ_1 expansion space $C_{\delta_1}^\infty = \{\boldsymbol{\delta}_1 : \delta_{1\boldsymbol{k}} \in (-\infty, +\infty), k = 1, 2\}$ and the vertex $P_{\delta_1}^j = \{\boldsymbol{\delta}_1 : |\delta_{1k}| = 1, k = 1, 2\}$ (j=1,2,3,4) of the symmetric convex domain $C_{\delta_1}^\infty = \{\delta_1 : |\delta_{1k}| \le 1, k = 1, 2\}$ formed by δ_1. These super radiation lines/ultra-rays are marked as $\delta_{11} = \pm\delta_{12}$, meeting the condition $\delta_1 \in C_{\delta_1} \subset C_{\delta_1}^\infty$.

(2) Add $\delta_{11} = \pm\delta_{12}$ to Equation 15 to solve the interval non-probabilistic reliability; two linear equations can be obtained. The interval non-probabilistic reliability set $\{\eta_{11}, \eta_{12}\}$ can be obtained by solved the two linear equations using the numerical method.

(3) The complex solutions are abandoned, and the absolute value of the real solution is selected. The minimum will be the interval non-probabilistic reliability η_1 of the jointed rockmass in an underground cavern.

In the same manner, when block slides along two structural planes i and j, as in (1), (2), and (3), the interval non-probabilistic reliability set can be solved, and the interval non-probabilistic reliability η_2 of the jointed rockmass in an underground cavern can be obtained from Equation 16.

V. APPLICATIONS IN THE JIAOJIA GOLD MINE

A. BRIEF INTRODUCTION TO THE JIAOJIA GOLD MINE

The Jiaojia gold mine, which is affiliated with the China National Gold Group Corporation, is a large gold deposit in China buried underground at more than 500 m and situated in the northeast of Laizhou City, Shandong Province. A certain roadway section of sublevel −470 in the Wangershan

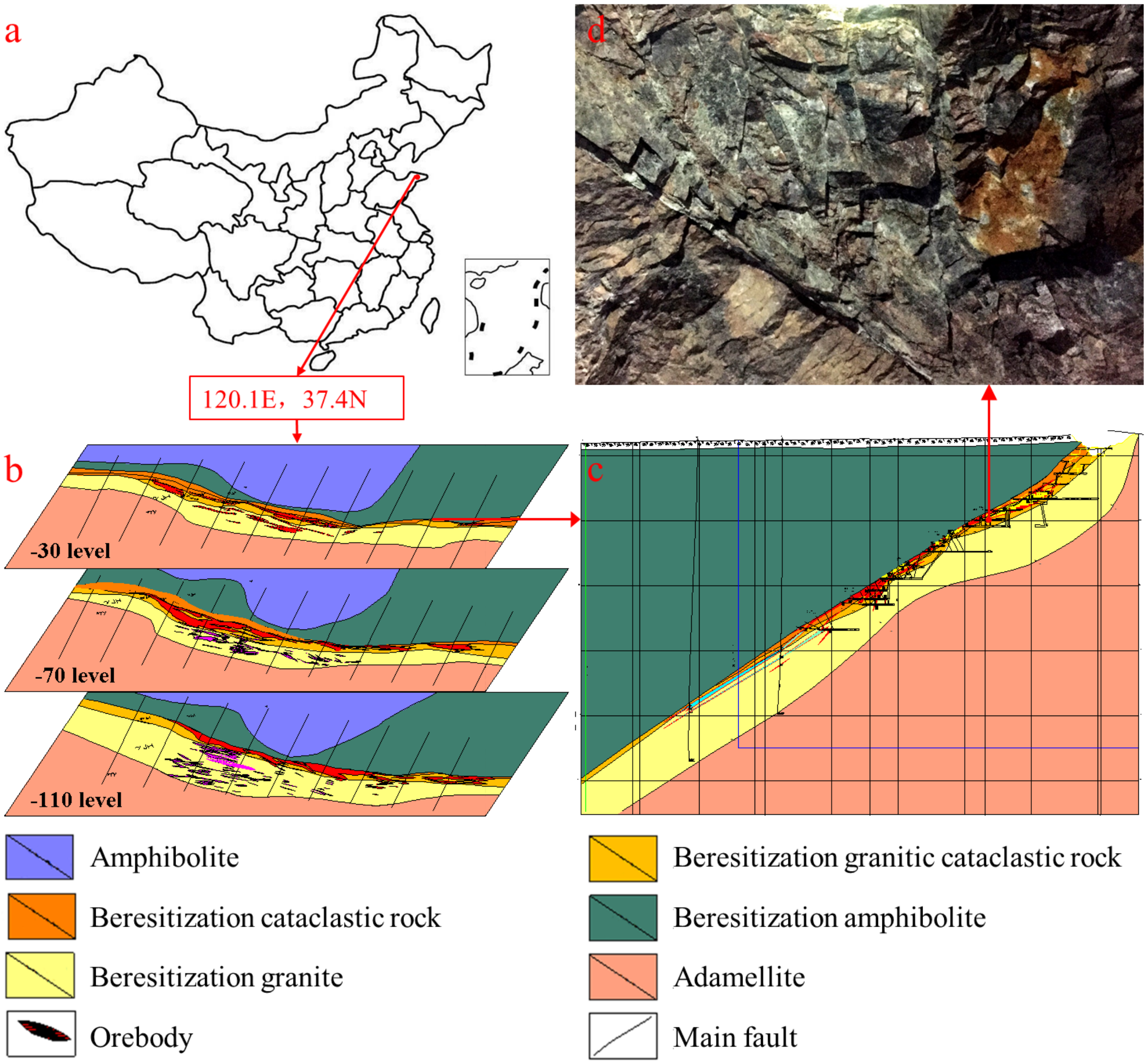

FIGURE 3. Sketch of Jiaojia gold mine: a The location, b The horizontal projection, c The vertical projection of line 120, and d The jointed rockmass of a certain tunnel.

mining area is a basket handle arch, which has a clear width of 4.2 m, and the heights of the vertical wall and the arch are 3 m and 1.4 m, respectively. The roadway has complex geological conditions with faults and developed joints. A large number of blocks are formed around the roadway because of the division of the structural planes. Disturbance of the blasting and excavation process may cause instability of these blocks. Instability of the blocks is not only a hidden danger to safety production but also a safety risk for the workers. The information of Jiaojia gold mine is shown in Fig 3. The preferred orientation can be divided into four groups according to the dip direction: the average dip direction and average dip angle of the first, second, third, and fourth groups are 13° and 76°, 300° and 79°, 113° and 61°, and 213° and 70°, respectively. The removable blocks under different joints combination can be assessed using block theory and the theorem of mobility. The safety factor, volume, weight, sliding mode, joint area, joint normal force, and sliding direction of each block can be calculated according to geometric principles and mechanical principles. These results are listed in Table 1; the block serial numbers are formed by the joint combinations and the block number of each joint combination; e.g., 1233 refers to the lower right block 3 of joint combination 123. A field investigation indicated that the sandwich materials of each group of structural planes differed from the other ones; the sandwich materials of the four groups are the intercalated layer, the crushing layer, the broken layer, and the brecciated broken layer. The interval shear strength parameters of each group of structural planes were obtained by consulting the relevant documents and performing statistical analyses, as listed in Table 2. The contour diagram for the joints, the rose diagram for the joint dip directions, the rose

TABLE 1. Relevant parameters of each block.

Joint combinations	Block numbers	Safety factor	Volume/ m^3	Weight /kN	Sliding mode	Joint areas /m^2	Joint normal forces/kN	Sliding direction
123	LR 3	13.42	0.12	3.32	joint 1 joint 3	0.45 0.23	0.33 1.84	81,57
	R 4	2.2	24.24	654.3	joint 1 joint 2	8.70 22.6	79.0 78.3	346,74
	F 5	S	41.72	1126				
	UL 6	FA	0.16	4.43				
124	F 3	S	4.33	116.9				
	UL 6	FA	3	80.98				
	UR 8	48.94	0	0.013	joint 2	0.01	0.001	314,79
134	F 1	S	2.7	72.85				
	LL 3	13.19	2.2	59.49	joint 1 joint 4	2.47 3.64	43.8 50.3	291,30
	LR 6	7.56	2.86	77.24	joint 3	4.53	42.5	100,60
	R 8	FA	0.7	18.99				
234	F 1	S	37.02	999.6				
	UL 3	6.24	1.53	41.33	joint 4	1.88	11.4	257,63
	LR 6	8.51	1.35	36.41	joint 3	2.43	20.1	100,60
	R 8	1.63	17.19	464.2	joint 2	14.2	37.3	314,79

Note: LR denotes the lower right block; R denotes the roof block; F denotes the floor block; UL denotes the upper left block; UR denotes the upper right block; LL denotes the lower left block.
S denotes stable; FA denotes a falling block.

TABLE 2. Interval shear strength parameters of the preferred planes.

Serial number of joints	Cohesive strength C/MPa	Internal friction angle φ/°	Friction coefficient f=tanφ
1	[0.005,0.03]	[8,14]	[0.14054,0.24933]
2	[0.02,0.06]	[16,22]	[0.28675,0.40403]
3	[0.03,0.1]	[26,31]	[0.48773,0.60086]
4	[0.04,0.15]	[33,40]	[0.64941,0.8391]

diagram for the joint dip angles, and the cluster analysis diagram for the joints are shown in Fig. 4.

The relationships between the maximum excavation area and the dip direction and dip angle of the roadway can be obtained through block theory; the relationships between the maximum block weight and the dip direction and dip angle can also be obtained. For the newly designed roadway, relation histograms, such as that in Fig. 5, can be drawn to seek the optimal solutions of the maximum excavation area and maximum block weight. To analyze the stability of a certain roadway after excavation, the Jiaojia gold mine is considered. The dip direction and dip angle of the roadway in this study is 190°∠22°. From Fig. 5, the maximum excavation area is approximately 40 m^2, and the block weight is approximately 820 kN. An excavation area that is sufficiently large can reduce the cost of the roadway support considerably, and a block weight that is sufficiently low is better for production safety. Considering these two aspects, the optimal dip direction of the roadway is approximately 15°, and the optimal dip angle is approximately 85°; however, this arrangement of the roadway is impractical, as the dip angle is excessively high for persons and equipments to pass through. Thus, when arranging a practical engineering project, the roadway should be designed to allow persons and equipments to pass through easily; however, such a design may cause the existence of many unstable blocks. Thus, all influencing factors should be considered in practical engineering; i.e., in addition to the maximum excavation area and block weight being considered, the interval non-probabilistic reliability should be combined with practical engineering to determine a reasonable

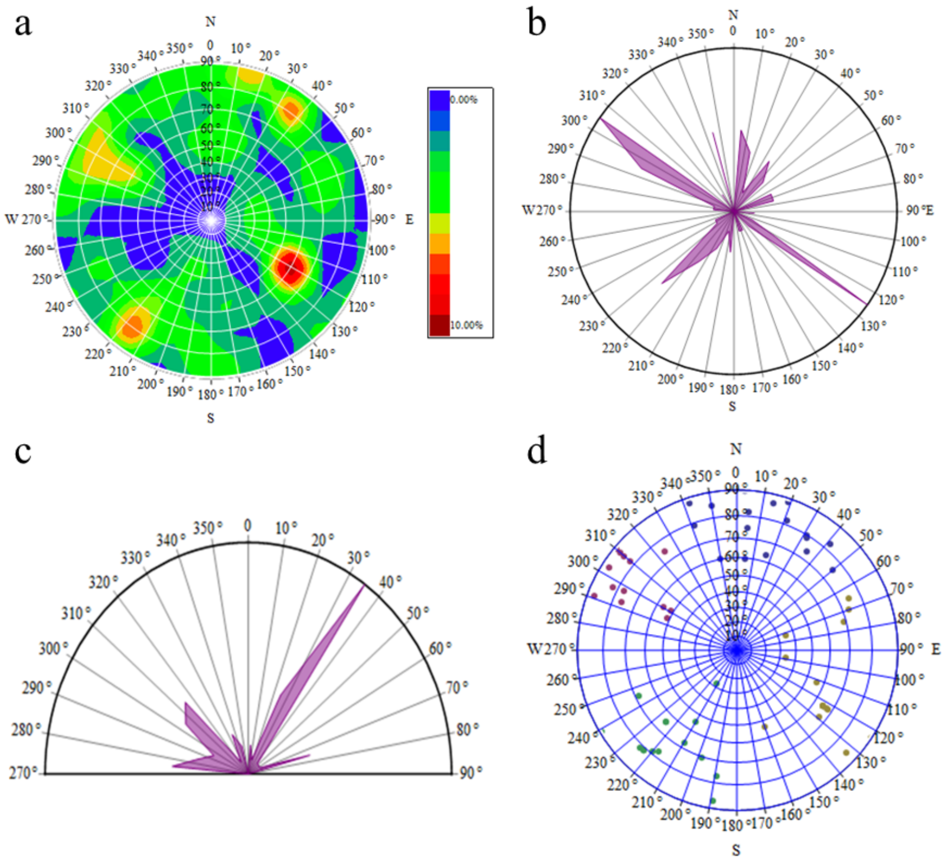

FIGURE 4. **Statistical characteristics of the dip angles and dip directions of the joints: a contour diagram for the joints; b rose diagram for the joint dip directions; c rose diagram for the joint dip angles, and d cluster analysis diagram for the jointed rockmass.**

orientation of the roadway. This is a complementary aspect of the case study in this article, aiming at explaining the function of block theory to analyze the maximum excavation area and maximum block weight; the focus of this article is to analyze the interval non-probabilistic reliability indexes of blocks.

B. RESULTS OF RANDOM RELIABILITY FOR KEY BLOCKS

The sliding condition of the key blocks can be divided into two types of situations according to block theory: sliding on a single structural plane and sliding on two structural planes. When a block is sliding on a single plane, the random reliability index is calculated according to Equation 4 and the interval non-probabilistic reliability is calculated according to Equation 15. When a block is sliding on two structural planes, the random reliability index is calculated according to Equation 10, and the interval non-probabilistic reliability is calculated according to Equation 16.

The mean values of $c_1, c_2, c_3, c_4, f_1, f_2, f_3$ and f_4 are 0.0175, 0.04, 0.065, 0.095, 0.194935, 0.34539, 0.544295 and 0.744255, respectively. The variation coefficients of $c_1, c_2, c_3, c_4, f_1, f_2, f_3$ and f_4 are 0.238095, 0.166667, 0.179487, 0.192982, 0.093014, 0.056593, 0.034641 and 0.042497, respectively. According to numerous studies [38], [39], c and f follow the normal distribution. Supposing that

$$X_1 = c_1 \sim N\left(0.0175, 4.17 \times 10^{-3}\right)$$
$$X_5 = f_1 \sim N\left(0.194935, 1.81 \times 10^{-2}\right)$$
$$X_2 = c_2 \sim N\left(0.04, 6.67 \times 10^{-3}\right)$$
$$X_6 = f_2 \sim N\left(0.34539, 1.95 \times 10^{-2}\right)$$
$$X_3 = c_3 \sim N\left(0.065, 1.17 \times 10^{-2}\right)$$
$$X_7 = f_3 \sim N\left(0.544295, 1.89 \times 10^{-2}\right)$$
$$X_4 = c_4 \sim N\left(0.095, 1.83 \times 10^{-2}\right)$$
$$X_8 = f_4 \sim N\left(0.744255, 3.16 \times 10^{-2}\right)$$

First-order reliability method is a method of linear approximation relative to each random variable of interest [40], a method to be most compatible with prevailing deterministic design technics [41].Considering that all of the variables follow normal distributions, the first-order reliability method can be used to calculate the random reliability. The MATLAB

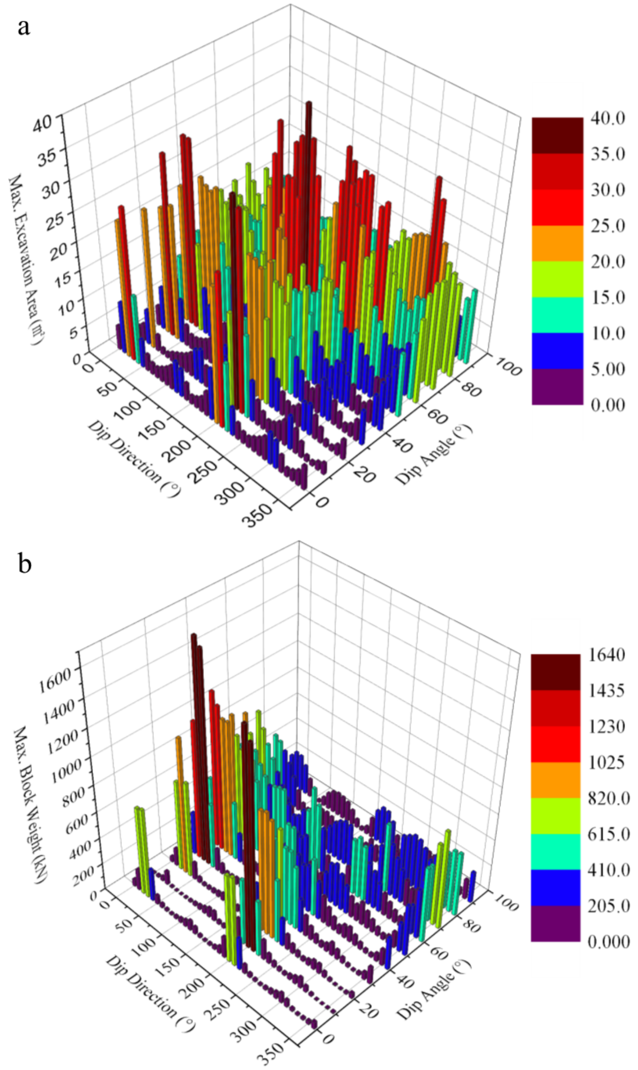

FIGURE 5. Maximum excavation areas and block weights for different dip angles and dip directions of the tunnels: a maximum excavation areas and b block weights.

software is applied to write a program to perform the calculations. The relevant parameters from Table 2 are determined and substituted into Equations 4 and 10 according to the different sliding modes. The specific process is listed in the appendix.

C. RESULTS OF INTERVAL NON-PROBABILISTIC RELIABILITY FOR KEY BLOCKS

Based on the theory above and the sliding mode of each block, the relevant parameters of a certain block from Table 2 are chosen and substituted into Equations 15 and 16 to calculate the interval non-probabilistic reliability separately. The specific process is also included in the appendix. The obtained safety factor, probabilistic reliability and interval non-probabilistic reliability of each block are listed in Table 3 to analyze consistency of the three reliability indexes. Table 3 reveals that the results for the traditional safety factor, random reliability, and interval non-probabilistic reliability are not entirely coincident. The results of 8 blocks of different joint combinations illustrates that the traditional safety factors are higher than the critical value of 1, indicating that all the blocks are stable. The results of random reliability are also greater than 0.96. It means that the stable probabilities are greater than 90%. With regard to the results for the interval non-probabilistic reliability, the results of block R4 of joint combination123 and block R8 of joint combination 234 are less than the critical value of 1, and the two blocks are in an unstable condition. Indeed, a roof falling disaster occurred in the position of the roadway that corresponds with our analysis. Thus, the analysis results of the interval non-probabilistic reliability indexes are in agreement with an actual situation. Analysis of the cause of this phenomenon illustrates that when calculating the random reliabilities, the distributions of the probability density are hypothetical because of the lack of field data; i.e., only 5 data points of samples are used to calculate the mean value and coefficient of variation, and the mean values are used to calculate the safety factors. In this case, it is difficult to accurately determine the parameters to calculate random reliabilities and safety factors. The uncertainties of the parameters are not fully considered when calculating the mean value, thus causing the deviation between the calculation results and actual situation when calculating the random reliabilities and safety factors. Therefore, it can be concluded that the proposed interval non-probabilistic reliability of jointed rockmass has three advantages. First, the calculated errors caused by uncertain mechanical parameters in traditional limit balance analysis can be avoided. Second, a strict data requirement is unnecessary because the uncertainty of the parameter value can be used when there is not a sufficient amount of data. Third, the sliding direction, sliding area, interval reliability of the key block and other relevant information can be analyzed using engineering data (including structural occurrence and mechanical parameters). The traditional probability reliability model includes the set of events as well as the probability density function of each event. Additional data are needed to accurately describe the probability distribution of parameters. In many cases of actual underground engineering, there is an insufficient amount of available data to determine the probability parameters of the variables, particularly in the stage of underground engineering design, because performing core drilling and a large number of indoor tests is cost-prohibitive. Under the artificial assumption of a distribution, the result of the probabilistic reliability calculation may not be valid, and the calculation is typically complex to perform. This situation has affected the practical application of the reliability method in underground engineering practice to a certain extent. However, the random reliability is undoubtedly extremely important, and the establishment of the interval non-probabilistic reliability of the surrounding jointed rockmass in underground engineering provides a beneficial complement to the random reliability method and does not mean to replace it. Random reliability is the preferred method when

TABLE 3. Safety factor, probabilistic reliability and interval non-probabilistic reliability of each block.

Joint combinations	Block numbers	Safety factor	Probabilistic reliability		Interval non-probabilistic reliability
			Reliability index	Random reliability	
123	LR 3	13.4210	6.4439	1.0000	1.5294
	R 4	2.2010	3.0244	0.9988	0.8225
	F 5	stable			
	UL 6	falling block			
124	F 3	stable			
	UL 6	falling block			
	UR 8	48.9370	5.8197	1.0000	1.9385
134	F 1	stable			
	LL 3	13.1880	5.9997	1.0000	1.7011
	LR 6	7.5570	4.7025	0.9999	1.5467
	R 8	falling block			
234	F 1	stable			
	UL3	6.2440	4.5184	0.9999	1.4809
	LR 6	8.5100	4.8093	0.9999	1.5838
	R 8	1.6280	1.5190	0.9356	0.4770

sufficient data are available to describe the uncertainty of the parameters; the interval non-probabilistic reliability model is appropriate when there is not a sufficient amount of data to determine the probability density distribution.

D. SENSITIVITY ANALYSIS OF EACH INTERVAL PARAMETER ON THE INTERVAL NON-PROBABILISTIC RELIABILITY

To compare and analyze the sensitivity of each interval parameter on the interval non-probabilistic reliability, make the deviation of parameters c and f of joints 1 and 2 of block 1234 and joint 2 of block 2348 change 0.002 toward both sides each time based on the previous deviation when calculating the interval non-probabilistic reliability indexes. The analysis process for block 1234 can be classified into 4 conditions:

(1) f_1^r c_2^r, and f_2^r are set as constant values, and c_1^r is set to 0.0025, 0.0045, 0.0065, 0.0085, 0.0105, 0.01255, 0.0145, 0.0165, 0.0185, 0.0205 and 0.0205. These values are substituted into Equation 16; Then, the corresponding interval non-probabilistic reliability indexes of block 1234 are obtained according to Equations 17 and 18. The changing regulations are shown in Fig. 6 **a**. A slight change in c_1^r can change the block stability considerably.

(2) c_1^r, c_2^r, and f_2^r are set as constant values, and f_1^r is set to 0.0444, 0.0464, 0.0484, 0.0504, 0.0524, 0.0544, 0.0564, 0.0584, 0.0604, 0.0624 and 0.0644. With the same solution as (1), the relationship between f_1^r and the interval non-probabilistic reliability indexes of block 1234 are obtained, as shown in Fig. 6 **a**. From Fig. 6 **a**, the relationship between f_1^r and the interval non-probabilistic reliability indexes is found to be a nearly linear dependence, and the changes in f_1^r have a minor effect on the interval non-probabilistic reliability indexes.

(3) c_1^r, f_1^r, and f_2^r are set as constant values, and c_2^r is set to 0.01, 0.012, 0.014, 0.016, 0.018, 0.022, 0.024, 0.026, 0.028 and 0.03. With the same solution as (1), the relationship between c_2^r and the interval non-probabilistic reliability indexes of block 1234 are obtained, as shown in Fig. 6 **b**. Fig. 6 **b** illustrates that the interval non-probabilistic reliability indexes are sensitive to changes in c_2^r: a minor change in c_2^r causes a considerable change in the interval non-probabilistic reliability indexes

(4) c_1^r, f_1^r, and c_2^r are set as constant values, and f_2^r is set to 0.0486, 0.0506, 0.0526, 0.0546, 0.0566, 0.0606, 0.0626, 0.0646, 0.0666 and 0.0686. With the same solution as (1), the relationship between f_2^r and the interval non-probabilistic reliability indexes of block 1234 are obtained, as shown in Fig. 6 **b**. Fig. 6 **b** illustrates that the relationship between f_2^r and the interval non-probabilistic reliability indexes is nearly linear and that changes of f_2^r have a minor effect on the interval non-probabilistic reliability indexes.

The analysis process for block 2348 can be classified into 2 conditions:

(1) f_2^r is set as a constant value, and c_2^r is set to 0.01, 0.012, 0.014, 0.016, 0.018, 0.022, 0.024, 0.026, 0.028 and 0.03. All of the values are substituted into Equation 15; the corresponding interval non-probabilistic reliability indexes of block 2348 are obtained according to Equations 17 and 18. The changing regulations are shown in Fig. 7. Fig. 7 illustrates that a slight change in c_2^r causes a considerable change in the block stability.

(2) c_2^r is set as a constant value, and f_2^r is set to 0.0486, 0.0506, 0.0526, 0.0546, 0.0566, 0.0606, 0.0626, 0.0646, 0.0666 and 0.0686. With the same solution as (1), the relationship between f_2^r and the interval non-probabilistic reliability indexes of block 2348 are obtained, as shown in Fig. 7. Fig. 7 illustrates that the relationship between f_2^r and the interval non-probabilistic reliability indexes is nearly linear, and the changes of f_2^r have a minor effect on the interval non-probabilistic reliability indexes.

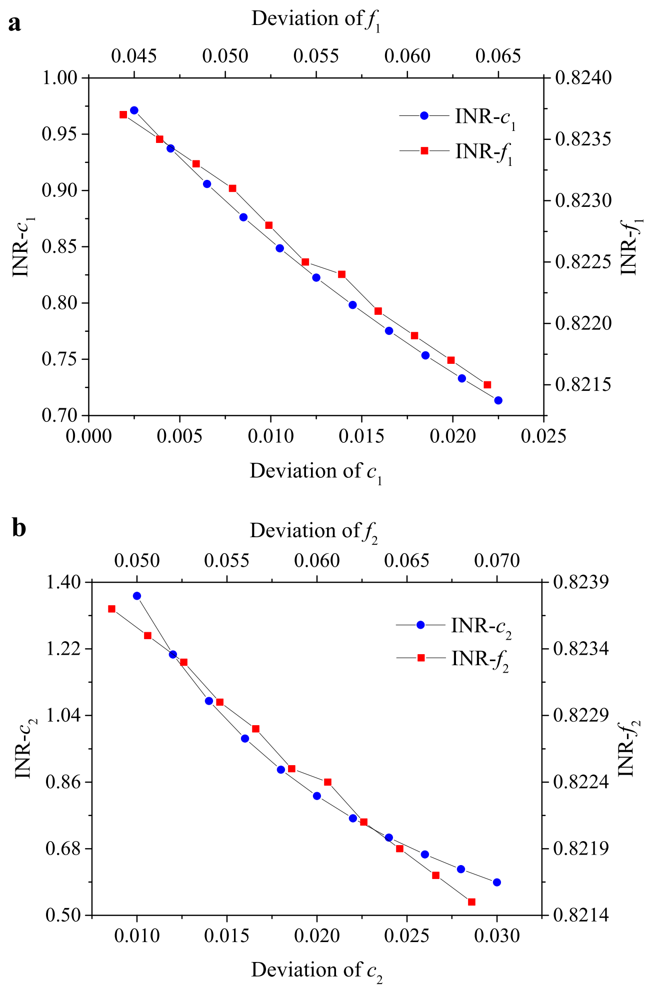

FIGURE 6. **Sensitivity analysis for the block 1234: a Deviation of c_1 (c_1^r) and f_1 (f_1^r), b Deviation of c_2 (c_2^r) and f_2 (f_2^r); INR indicates the interval non-probabilistic reliability.**

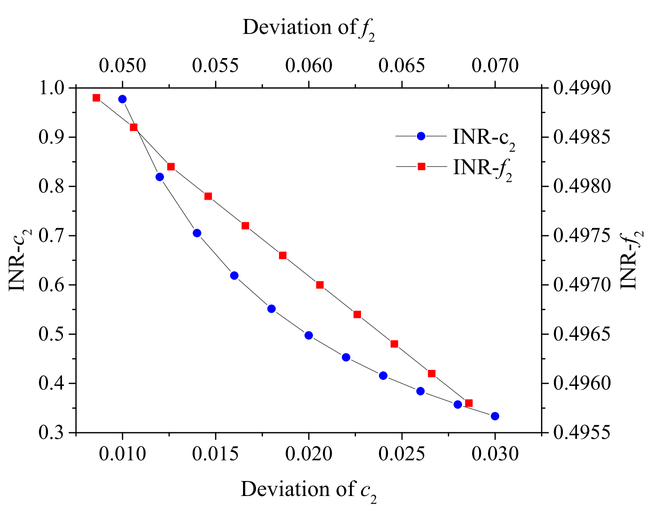

FIGURE 7. **Sensitivity analysis for block 2348: Deviation of c_2 (c_2^r) and Deviation of f_2 (f_2^r); INR indicates the interval non-probabilistic reliability.**

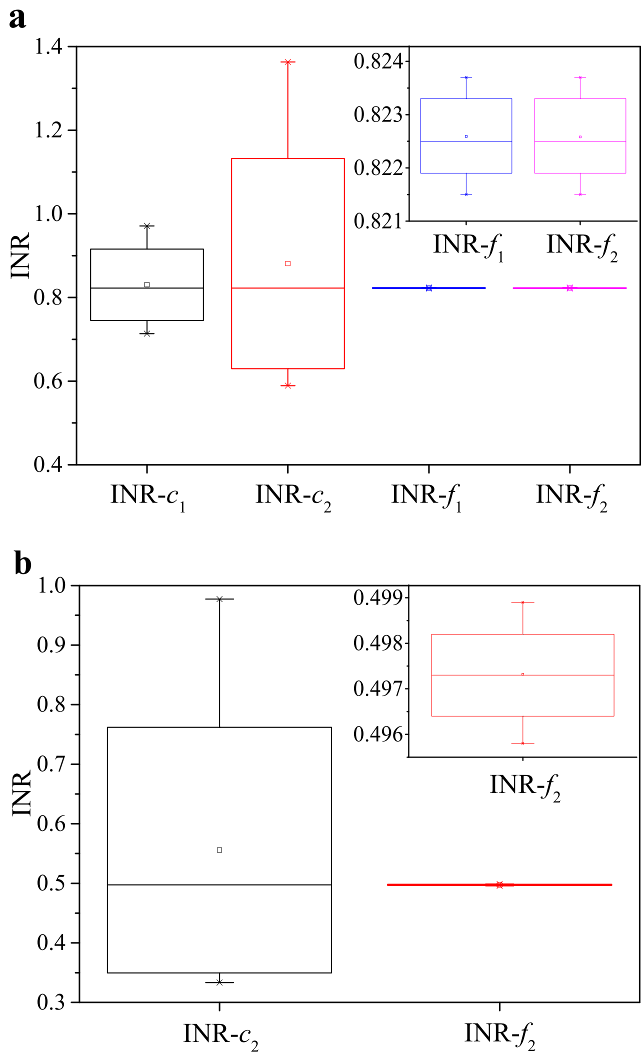

FIGURE 8. **Box charts for INRs under changes of c and f: a results for block 1234, b results for block 2348.**

Fig. 6 and Fig. 7show that the effects of c_1^r and c_2^r on the interval non-probabilistic reliability are greater than those of f_1^r and f_2^r. Slight changes in c_1^r and c_2^r can cause a considerable difference in the interval non-probabilistic reliability and thus dramatically affects the state of the block. From this perspective, a limitation of the traditional limit balance analysis is that the values of certain parameters are strictly required during the calculation process. In fact, it is difficult to obtain a definite and reliable value, whereas it is relatively easy to obtain a specific range of the parameter; this ease is one of the major advantages of the interval non-probabilistic reliability.

The relationship between shear strength (c and f) and the interval non-probabilistic reliability can be obtained through the box charts in Fig. 8. From Fig. 8 **a** and **b**, it can be also clearly seen that the interval non-probabilistic reliability is more sensitive to the change of c than to the change of f. It also can be found from Fig. 8 **a** that c_2 has a greater effect on the interval non-probabilistic reliability than that of c_1. Therefore, it is necessary to firstly focus on supported works for the specified direction, which is perpendicular to joint 2. It also gives us an important guidance that the weakest joint of multiple joints should be given priority to conduct support works.

VI. CONCLUSION

A new interval non-probabilistic reliability measurement and analysis method for a jointed rockmass in underground engineering was proposed based on the interval model and block theory. This proposed method requires knowledge of the bounds of the uncertain parameters but not their specific distributions. As a result, the initial data requirements are reduced considerably.

The developed interval non-probabilistic reliability method was used to evaluate the stability of the rockmass in the Jiaojia gold mine. The calculation results of the interval non-probabilistic reliability were found to be in agreement with an actual situation. It can be concluded that the interval non-probabilistic reliability method is applicable when the amount of data is scarce.

The most sensitive mechanical parameters and sliding direction of the key block can be determined through an analysis of the sensitivity of the mechanical parameters towards the interval non-probabilistic reliability, thereby providing instructions for the excavation and support of the underground cavern.

It is noted that the non-probabilistic reliability method is not designed to replace the probabilistic reliability method but instead serves as a useful complement to the probabilistic reliability and the safety factor methods. The probability reliability method can be used when there is a sufficient amount of data to describe the probability properties of the uncertain parameters, and the interval non-probabilistic reliability models can be used when the uncertainty in the data is reduced.

APPENDIX

1 The specific process and the results of random reliability are as follows:

Substitute the relevant parameters of each removable block which sliding on a single structural plane into Equation 4, and the relevant parameters of each removable block which sliding on two structural planes into Equation 10. Solve the obtained equations:

For block 1233:

$$\begin{aligned} g\left(\varphi_i, \varphi_j, c_i, c_j\right) &= N_i \tan\varphi_i + N_j \tan\varphi_j + c_i S_i + c_j S_j - W \sin\alpha \\ &= 0.0003 \tan\varphi_i + 0.0018 \tan\varphi_j + 0.45 c_i \\ &\quad + 0.23 c_j - 0.0033 \sin 57^\circ = 0 \end{aligned}$$

The equation to calculating the random reliability index is solved, and the result is $\beta = 6.4439$.

$$P_s = 1 - \Phi(-\beta) = \Phi(\beta) = 1$$

For block 1234:

$$\begin{aligned} g\left(\varphi_i, \varphi_j, c_i, c_j\right) &= N_i \tan\varphi_i + N_j \tan\varphi_j + c_i S_i + c_j S_j - W \sin\alpha \\ &= 0.0791 \tan\varphi_i + 0.0783 \tan\varphi_j + 8.7 c_i + 22.55 c_j \\ &\quad - 0.6543 \sin 74^\circ = 0 \end{aligned}$$

The equation to calculating the random reliability index is solved, and the result is β= 3.0244.

$$P_s = 1 - \Phi(-\beta) = \Phi(\beta) = 0.9988$$

For block 1248:

$$\begin{aligned} g(\varphi, c) &= W \cos\alpha \tan\varphi + cS - W \sin\alpha \\ &= 2.48 \times 10^{-6} \tan\varphi + 0.01c - 1.28 \times 10^{-5} = 0 \end{aligned}$$

The equation to calculating the random reliability index is solved, and the result is $\beta = 5.8197$.

$$P_s = 1 - \Phi(-\beta) = \Phi(\beta) = 1$$

For block 1343:

$$\begin{aligned} g\left(\varphi_i, \varphi_j, c_i, c_j\right) &= N_i \tan\varphi_i + N_j \tan\varphi_j + c_i S_i + c_j S_j - W \sin\alpha \\ &= 0.0438 \tan\varphi_i + 0.0503 \tan\varphi_j + 2.47 c_i \\ &\quad + 3.64 c_j - 0.0595 \sin\ 30^\circ = 0 \end{aligned}$$

The equation to calculating the random reliability index is solved, and the result is $\beta = 5.9997$.

$$P_s = 1 - \Phi(-\beta) = \Phi(\beta) = 1$$

For block 1346:

$$\begin{aligned} g(\varphi, c) &= W \cos\alpha \tan\varphi + cS - W \sin\alpha \\ &= 0.0386 \tan\varphi + 4.53c - 0.0669 = 0 \end{aligned}$$

The equation to calculating the random reliability index is solved, and the result is $\beta = 4.7025$.

$$P_s = 1 - \Phi(-\beta) = \Phi(\beta) = 0.9999$$

For block 1343:

$$\begin{aligned} g(\varphi, c) &= W \cos\alpha \tan\varphi + cS - W \sin\alpha \\ &= 0.01875 \tan\varphi + 1.88c - 0.0368 = 0 \end{aligned}$$

The equation to calculating the random reliability index is solved, and the result is $\beta = 4.5184$.

$$P_s = 1 - \Phi(-\beta) = \Phi(\beta) = 0.9999$$

For block 2346:

$$\begin{aligned} g(\varphi, c) &= W \cos\alpha \tan\varphi + cS - W \sin\alpha \\ &= 0.0182 \tan\varphi + 2.43c - 0.0315 = 0 \end{aligned}$$

The equation to calculating the random reliability index is solved, and the result is $\beta = 4.8093$.

$$P_s = 1 - \Phi(-\beta) = \Phi(\beta) = 0.9999$$

For block 2348:

$$\begin{aligned} g(\varphi, c) &= W \cos\alpha \tan\varphi + cS - W \sin\alpha \\ &= 0.0886 \tan\varphi + 14.23c - 0.45567 = 0 \end{aligned}$$

The equation to calculating the random reliability index is solved, and the result is $\beta = 1.5190$.

$$P_s = 1 - \Phi(-\beta) = \Phi(\beta) = 0.9356$$

2 The specific process and results of non-probabilistic reliability are as follows.

Substitute the relevant parameters of each removable block which sliding on a single structural plane into Equation 15, and the relevant parameters of each removable block which sliding on two structural planes into Equation 16. Solve the obtained equations:

For block 1233:

$$\begin{aligned} Z_2 &= g(\delta_2) = \left(c_i^c + c_i^r\delta_{ci}\right)S_i + \left(c_j^c + c_j^r\delta_{cj}\right)S_j + N_i\left(f_i^c + f_i^r\delta_{\varphi i}\right) \\ &\quad + N_j\left(f_j^c + f_j^r\delta_{\varphi j}\right) - W\sin\theta = \left(0.0175 + 0.0125\delta_{c_i}\right)0.45 \\ &\quad + \left(0.065 + 0.035\delta_{c_j}\right)0.23 + 0.0003\left(0.1949 + 0.0544\delta_{\varphi_i}\right) \\ &\quad + 0.0018\left(0.5443 + 0.0566\delta_{\varphi_j}\right) - 0.0033\sin 57^\circ = 0 \end{aligned}$$

The equation to calculating the interval non-probabilistic reliability is solved, and the result is

$$\beta = 1.5294$$

For block 1234:

$$\begin{aligned} Z_2 &= g(\delta_2) = \left(c_i^c + c_i^r\delta_{ci}\right)S_i + \left(c_j^c + c_j^r\delta_{cj}\right)S_j + N_i\left(f_i^c + f_i^r\delta_{\varphi i}\right) \\ &\quad + N_j\left(f_j^c + f_j^r\delta_{\varphi j}\right) - W\sin\theta = \left(0.0175 + 0.0125\delta_{c_i}\right)8.7 \\ &\quad + \left(0.04 + 0.02\delta_{c_j}\right)22.55 + 0.0791\left(0.1949 + 0.0544\delta_{\varphi_i}\right) \\ &\quad + 0.0783\left(0.3454 + 0.0586\delta_{\varphi_j}\right) - 0.6543\sin 74^\circ = 0 \end{aligned}$$

The equation to calculating the interval non-probabilistic reliability is solved, and the result is

$$\beta = 0.8225$$

For block 1248:

$$\begin{aligned} Z_1 &= g(\delta_1) = W\cos\alpha\tan\left(\varphi_i^c + \varphi_i^r\delta_{\varphi i}\right) \\ &\quad + \left(c_i^c + c_i^r\delta_{ci}\right)S - W\sin\alpha \\ &= 0.000013\cos 79^\circ\left(0.3454 + 0.0586\delta_{\varphi_i}\right) \\ &\quad + \left(0.04 + 0.02\delta_{c_i}\right)0.01 - 0.000013\sin 79^\circ = 0 \end{aligned}$$

The equation to calculating the interval non-probabilistic reliability is solved, and the result is

$$\beta = 1.9385$$

For block 1343:

$$\begin{aligned} Z_2 &= g(\delta_2) = \left(c_i^c + c_i^r\delta_{ci}\right)S_i + \left(c_j^c + c_j^r\delta_{cj}\right)S_j \\ &\quad + N_i\left(f_i^c + f_i^r\delta_{\varphi i}\right) + N_j\left(f_j^c + f_j^r\delta_{\varphi j}\right) - W\sin\theta \\ &= \left(0.0175 + 0.0125\delta_{c_i}\right)2.47 \\ &\quad + \left(0.095 + 0.055\delta_{c_j}\right)3.64 \\ &\quad + 0.0438\left(0.1949 + 0.0544\delta_{\varphi_i}\right) \\ &\quad + 0.0503\left(0.7443 + 0.0948\delta_{\varphi_j}\right) - 0.0595\sin 30^\circ = 0 \end{aligned}$$

The equation to calculating the interval non-probabilistic reliability is solved, and the result is

$$\beta = 1.7011$$

For block 1346:

$$\begin{aligned} Z_1 &= g(\delta_1) = W\cos\alpha\left(f_i^c + f_i^r\delta_{\varphi i}\right) + \left(c_i^c + c_i^r\delta_{ci}\right)S - W\sin\alpha \\ &= 0.0772\cos 60^\circ\left(0.5443 + 0.0566\delta_{\varphi_i}\right) \\ &\quad + \left(0.065 + 0.035\delta_{c_i}\right)4.53 - 0.0772\sin 60^\circ = 0 \end{aligned}$$

The equation to calculating the interval non-probabilistic reliability is solved, and the result is

$$\beta = 1.5467$$

For block 2343:

$$\begin{aligned} Z_1 &= g(\delta_1) = W\cos\alpha\left(f_i^c + f_i^r\delta_{\varphi i}\right) \\ &\quad + \left(c_i^c + c_i^r\delta_{ci}\right)S - W\sin\alpha \\ &= 0.0413\cos 63^\circ\left(0.7443 + 0.0948\delta_{\varphi_i}\right) \\ &\quad + \left(0.095 + 0.055\delta_{c_i}\right)1.88 - 0.0413\sin 63^\circ = 0 \end{aligned}$$

The equation to calculating the interval non-probabilistic reliability is solved, and the result is

$$\beta = 1.4809$$

For block 2346:

$$\begin{aligned} Z_1 &= g(\delta_1) = W\cos\alpha\left(f_i^c + f_i^r\delta_{\varphi i}\right) \\ &\quad + \left(c_i^c + c_i^r\delta_{ci}\right)S - W\sin\alpha \\ &= 0.0364\cos 60^\circ\left(0.5443 + 0.0566\delta_{\varphi_i}\right) \\ &\quad + \left(0.065 + 0.035\delta_{c_i}\right)2.43 - 0.0364\sin 60^\circ = 0 \end{aligned}$$

The equation to calculating the interval non-probabilistic reliability is solved, and the result is

$$\beta = 1.5838$$

For block 2348:

$$\begin{aligned} Z_1 &= g(\delta_1) = W\cos\alpha\tan\left(f_i^c + f_i^r\delta_{\varphi i}\right) \\ &\quad + \left(c_i^c + c_i^r\delta_{ci}\right)S - W\sin\alpha \\ &= 0.4642\cos 79^\circ\left(0.3454 + 0.0586\delta_{\varphi_i}\right) \\ &\quad + \left(0.04 + 0.02\delta_{c_i}\right)14.23 - 0.4642\sin 79^\circ = 0 \end{aligned}$$

The equation to calculating the interval non-probabilistic reliability is solved, and the result is

$$\beta = 0.4973$$

REFERENCES

[1] R. E. Goodman and G. H. Shi, *Block Theory and Its Application to Rock Engineering*. Englewood Cliffs, NJ, USA: Prentice-Hall, 1985.

[2] L. J. Dong, and X. B. Li, "Comprehensive models for evaluating rockmass stability based on statistical comparisons of multiple classifiers," *Math. Problems Eng.*, vol. 2013, Aug. 2013, Art. no. 395096.

[3] G. H. Shi, "Geometrical approach of rock mass stabilization in rock mass stability analysis," *Sci China*, vol. 1981, no. 4, pp. 487–495, Apr. 1981.

[4] J. T. Christian, C. C. Ladd, and G. Baecher, "Reliability applied to slope stability analysis," *J. Geotech. Eng.*, vol. 120, no. 12, pp. 2180–2207, Dec. 1994.

[5] R. N. Chowdhury and D. W. Xu, "Geotechnical system reliability of slopes," *Reliab. Eng. Syst. Saf.*, vol. 47, no. 3, pp. 141–151, Jan. 1995.
[6] A. T. C. Goh, "Deterministic and reliability assessment of basal heave stability for braced excavations with jet grout base slab," *Eng. Geol.*, vol. 218, pp. 63–69, Feb. 2017.
[7] A. T. C. Goh and W. Zhang, "Reliability assessment of stability of underground rock caverns," *Int. J. Rock Mech. Mining Sci.*, vol. 55, pp. 157–163, Oct. 2012.
[8] J. M. Duncan, "Factors of safety and reliability in geotechnical engineering," *J. Geotech. Geoenviron. Eng.*, vol. 126, no. 4, pp. 307–316, Apr. 2000.
[9] D. Q. Li, X. S. Tang, and K. K. Phoon, "Bootstrap method for characterizing the effect of uncertainty in shear strength parameters on slope reliability," *Reliab. Eng. Syst. Saf.*, vol. 140, pp. 99–106, Aug. 2015.
[10] J. Qiu, Y. Wei, and L. Wu, "A novel approach to reliable control of piecewise affine systems with actuator faults," *IEEE Trans. Circuits Syst. II, Exp. Briefs*, vol. 64, no. 8, pp. 957–961, Aug. 2017.
[11] Y. Wei, J. Qiu, and H. R. Karimi, "Reliable output feedback control of discrete-time fuzzy affine systems with actuator faults," *IEEE Trans. Circuits Syst. I, Reg. Papers*, vol. 64, no. 1, pp. 170–181, Jan. 2017.
[12] Y. Wei, J. Qiu, H. Lam, and L. Wu, "Approaches to T–S fuzzy-affine-model-based reliable output feedback control for nonlinear Ito stochastic systems," *IEEE Trans. Fuzzy Syst.*, vol. 25, no. 3, pp. 569–583, Jun. 2017.
[13] I. Elishakoff, "Uncertainties in mechanical structures: AMF reudenthal's criticisms and modern convex models," *J. Appl. Mech.*, vol. 63, no. 1, pp. 683–692, 1999.
[14] M. L. Beconcini, P. Croce, F. Marsili, M. Muzzi, and E. Rosso, "Probabilistic reliability assessment of a heritage structure under horizontal loads," *Probab. Eng. Mech.*, vol. 45, pp. 198–211, Jul. 2016.
[15] T. Xiao, D. Q. Li, Z. J. Cao, S. K. Au, and K. K. Phoon, "Three-dimensional slope reliability and risk assessment using auxiliary random finite element method," *Comput. Geotech.*, vol. 79, pp. 146–158, Oct. 2016.
[16] T. L. L. Orr, "Defining and selecting characteristic values of geotechnical parameters for designs to eurocode 7," *Georisk, Assessment Manage. Risk Eng. Syst. Geohazards*, vol. 11, no. 1, pp. 103–115, Nov. 2016.
[17] G. A. Fenton and D. V. Griffiths, *Risk Assessment in Geotechnical Engineering*. New York, NY, USA: Wiley, 2008.
[18] D. V. Griffiths, J. Huang, and G. A. Fenton, "On the reliability of earth slopes in three dimensions," *Proc. R. Soc. London A, Math., Phys. Eng. Sci.*, vol. 465, pp. 3145–3164, Jul. 2009.
[19] D. V. Griffiths, J. Huang, and G. A. Fenton, "Probabilistic infinite slope analysis," *Comput. Geotech.*, vol. 38, no. 4, pp. 577–584, Jun. 2011.
[20] S.-H. Jiang, D.-Q. Li, Z.-J. Cao, C.-B. Zhou, and K.-K. Phoon, "Efficient system reliability analysis of slope stability in spatially variable soils using Monte Carlo simulation," *J. Geotech. Geoenviron. Eng.*, vol. 141, no. 2, pp. 04014096-1–04014096-13, Feb. 2015.
[21] D.-Q. Li, X.-H. Qi, Z.-J. Cao, X.-S. Song, K.-K. Phoon, and C.-B. Zhou, "Evaluating slope stability uncertainty using coupled Markov chain," *Comput. Geotech.*, vol. 73, pp. 72–82, Mar. 2016.
[22] X.-H. Tan, W.-H. Bi, X.-L. Hou, and W. Wang, "Reliability analysis using radial basis function networks and support vector machines," *Comput. Geotech.*, vol. 38, no. 2, pp. 178–186, Mar. 2011.
[23] D.-Q. Li, D. Zheng, Z.-J. Cao, X.-S. Tang, and K.-K. Phoon, "Response surface methods for slope reliability analysis: Review and comparison," *Eng. Geol.*, vol. 203, pp. 3–14, Mar. 2015.
[24] Q. Lü and B. K. Low, "Probabilistic analysis of underground rock excavations using response surface method and SORM," *Comput. Geotech.*, vol. 38, no. 8, pp. 1008–1021, Dec. 2011.
[25] B. K. Low, J. Zhang, and W. H. Tang, "Efficient system reliability analysis illustrated for a retaining wall and a soil slope," *Comput. Geotech.*, vol. 38, no. 2, pp. 196–204, Mar. 2011.
[26] N. Dadashzadeh, H. S. B. Duzgun, and N. Yesiloglu-Gultekin, "Reliability-based stability analysis of rock slopes using numerical analysis and response surface method," *Rock Mech. Rock Eng.*, vol. 50, no. 8, pp. 2119–2133, Mar. 2017, doi: 10.1007/s00603-017-1206-2.
[27] W. Zhang and A. T. C. Goh, "Reliability assessment on ultimate and serviceability limit states and determination of critical factor of safety for underground rock caverns," *Tunnelling Underground Space Technol.*, vol. 32, pp. 221–230, Nov. 2012.
[28] S. X. Guo and Z. Z. Lü, "A non-probabilistic robust reliability method for analysis and design optimization of structures with uncertain-but-bounded parameters," *Appl. Math. Model.*, vol. 39, no. 7, pp. 1985–2002, Apr. 2015.
[29] B. Y. Ni, C. Jiang, and X. Han, "An improved multidimensional parallelepiped non-probabilistic model for structural uncertainty analysis," *Appl. Math. Model.*, vol. 40, nos. 7–8, pp. 4727–4745, Apr. 2016.
[30] H. Su, J. Li, Z. P. Wen, and Z. Fu, "Dynamic non-probabilistic reliability evaluation and service life prediction for arch dams considering time-varying effects," *Appl. Math. Model.*, vol. 40, nos. 15–16, pp. 6908–6923, Aug. 2016.
[31] D. Wu, W. Gao, F. Tin-Loi, and Y. L. Pi, "Probabilistic interval limit analysis for structures with hybrid uncertainty," *Eng. Struct.*, vol. 114, pp. 195–208, May 2016.
[32] M. S. Chowdhury, C. Song, W. Gao, and C. Wang, "Reliability analysis of homogeneous and bimaterial cracked structures by the scaled boundary finite element method and a hybrid random-interval model," *Struct. Saf.*, vol. 59, pp. 53–66, Mar. 2016.
[33] Y. Ben-Haim, S. Cogan, and L. Sanseigne, "Usability of mathematical models in mechanical decision processes," *Mech. Syst. Signal Process.*, vol. 12, no. 1, pp. 121–134, Jan. 1998.
[34] S. Guo, "A non-probabilistic model of structural reliability based on interval analysis," *Chin. J. Comput. Mech.*, vol. 18, no. 1, pp. 56–60, Jan. 2001.
[35] T. Jiang, J. J. Chen, P. G. Jiang, and Y. F. Tuo, "A one-dimensional optimization algorithm for non-probabilistic reliability index," *Eng. Mech.*, vol. 24, no. 7, pp. 23–27, Jul. 2007.
[36] G. Alefeld and G. Mayer, "Interval analysis: Theory and applications," *J. Comput. Appl. Math.*, vol. 121, nos. 1–2, pp. 421–464, Sep. 2000.
[37] L. J. Dong, D. Y. Sun, and X. B. Li, "Theoretical and case studies of interval nonprobabilistic reliability for tailing dam stability," *Geofluids*, vol. 2017, Aug. 2013, Art. no. 8745894.
[38] H. Manchao, S. Yonghua, and J. Haihe, "Reliability analysis model of blocky rockmass stability and its application," *Chin. J. Rock Mech. Eng.*, vol. 21, no. 3, pp. 343–348, Mar. 2002.
[39] F. Q. Gong, T. L. Huang, and X. B. Li, "Research on approximation method and discriminative criterion of the optimal probability distribution of geotechnical parameters," *Chin. J. Rock Mech. Eng.*, vol. 35, no. 12, pp. 2452–2460, Dec. 2016.
[40] H. Bonstrom and R. B. Corotis, "Building portfolio seismic loss assessment using the first-order reliability method," *Struct. Saf.*, vol. 52, pp. 113–120, Jan. 2015.
[41] V. Verderaime, "Illustrated structural application of universal first-order reliability method," NASA, Washington, DC, USA, Tech. Rep. 3501, Sep. 1994.

LONGJUN DONG (M'16) received the Ph.D. degree from the School of Resources and Safety Engineering, Central South University, Changsha, China, in 2013. From 2012 to 2013, he was an Assistant Researcher with the Australia Center for Geomechanics, The University of Western Australia, Perth, Australia. His current research interests include computational methods in location and identification for shock sources, seismic signals, machine learning algorithms, and rock/ mineral mechanics for mining science.

He is currently an Associate Professor with the School of Resources and Safety Engineering, Central South University. He is a member of the ASCE and ISRM. He is invited to serve as the Editorial Board Member of Scientific Reports, the Internal Journal of Distributed Sensor Networks, and Shock and Vibration. He was selected for the Young Elite Scientists Sponsorship Program by the China Association for Science and Technology. He has served as a reviewer of over 30 journals.

DAOYUAN SUN received the B.Sc. degree in mining engineering from Central South University, Changsha, China, in 2015, where he is currently pursuing the M.Sc. degree. His research interests include rock mechanics, reliability analysis, microseismic monitoring, and microseismic/AE source locating method.

XIBING LI received the Ph.D. degree in mining engineering from the Central South University of Technology, Changsha, China, in 1992. He was a Senior Visiting Scholar with the Rock Mechanics and Explosives Research Center, University of Missouri Rolla, from 1998 to 1999. He was also a Researcher with NanYang Technological University, Singapore, from 1999 to 2001. He received four projects of the National Science and Technology Awards, and 14 projects of Provincial/Ministerial Science and Technology Awards. He was selected for The National Science Fund for Distinguished Young Scholars and the Chang Jiang Distinguished Professor. He received awards, including the National Award for Youth in Science and Technology and the National Excellent Scientific and Technological Worker.

Dr. Li has been a Committee Member of Rock Dynamics of International Society for Rock Mechanics since 2008. He has also been the Vice-President of the Chinese Society for Rock Mechanics and Engineering since 2016.

ZILONG ZHOU received the Ph.D. degree from Central South University, Changsha, China, in 2007. Then he became an Associate Professor in 2009. From 2011 to 2012, he was a Visiting Professor with Toronto University, Canada. He is currently a Professor and Vice-Dean of the School of Resources and Safety Engineering, Central South University. He is the Principal Scientist of the National Basic Research Program of China, the Cheung Kong Young Scholar of Chinese Department of Education, and also the Project Leader of the National Outstanding Youth Fund of China. He has authored over 100 papers published in academic journals. His current research interests include rock dynamics, rock burst monitoring and prevention, mine collapse mechanism, and disaster control.

Dr. Zhou is a member of the Rock Dynamic Commission of the International Society for Rock Mechanics, and the Executive Member of the Chinese Society for Rock Mechanics and Engineering. He received the national prize of scientific and technological progress, provincial prize of natural science, provincial excellent doctor degree dissertation, and three other ministerial level awards. He has served as the chair or co-chair for almost ten conference/workshops and technical forums.